

**THE GOVERNMENT OF SULTANATE OF OMAN**

**HYDROLOGIC OBSERVATION PROJECT  
IN THE BATINAH COAST  
OF SULTANATE OF OMAN**

**FINAL REPORT**

**VOLUME 4**

**SUPPORTING REPORT III**

- F. REMOTE SENSING**
- G. HYDROLOGIC WATER BALANCE IN THE PROJECT AREA**
- H. MISCELLANEOUS**

**MARCH 1986**

**JAPAN INTERNATIONAL COOPERATION AGENCY**

RY



JICA LIBRARY



1040285173



**THE GOVERNMENT OF SULTANATE OF OMAN**

**HYDROLOGIC OBSERVATION PROJECT  
IN THE BATINAH COAST  
OF SULTANATE OF OMAN**

**FINAL REPORT**

**VOLUME 4**

**SUPPORTING REPORT III**

**F. REMOTE SENSING**

**G. HYDROLOGIC WATER BALANCE IN THE PROJECT AREA**

**H. MISCELLANEOUS**

**MARCH 1986**

**JAPAN INTERNATIONAL COOPERATION AGENCY**

国際協力事業団		
受入 月日	'87.10.15	310
登録 No.	16890	61.7 SDS

**SUPPORTING REPORT F**

**REMOTE SENSING**





## TABLE OF CONTENTS

	<u>Page</u>
<b>CHAPTER 1    LANDSAT IMAGE ANALYSIS</b>	
1.1    Objectives and Methods .....	F-1
1.2    Creation of Color Synthesized Images (False Color) .....	F-2
1.3    Surface Covering Classification .....	F-4
1.3.1    Surface Covering Classified Images .....	F-4
1.3.2    Features of Each Wadi from the Classified Images .....	F-5
1.3.3    Result of Classification of Dense and Sparse Vegetation .....	F-6
1.3.4    Area Accounting .....	F-9
1.3.5    Correspondence between the Classified Images and Air Photos .....	F-12
1.4    Vegetation Distribution .....	F-14
1.4.1    Vegetation Distribution Periodic Series Change Images .....	F-14
1.4.2    Features of the Time Series Change Pattern Diagrams .....	F-14
1.4.3    By-band Ratio Images .....	F-16
1.5    Albedo Images .....	F-18
1.5.1    Albedo Images .....	F-18
1.5.2    Albedo Image-Quadrature .....	F-18
1.6    Analysis Image Processing for the Topographic and Geological Survey .....	F-21
1.6.1    Result of Analysis Image .....	F-21
1.6.2    Principle Component Analysis Images .....	F-21
1.6.3    Features of the Study Area based on the Analysis Results .....	F-24
 <b>CHAPTER 2    NOAA RAINFALL DISTRIBUTION ANALYSIS</b>	
2.1    Objectives and Methods .....	F-28
2.2    Image Processing .....	F-29
2.3    Features of Each Rainfall .....	F-34

	<u>Page</u>
2.4 Rainfall Distribution Analysis .....	F-36
2.5 Results of Rainfall Distribution Analysis.....	F-38
2.5.1 Days when Rainfall was observed.....	F-38
2.5.2 Days when Rainfall was not observed only at a few sites .....	F-41
 <b>CHAPTER 3 NOAA IMAGE ANALYSIS ON SOIL MOISTURE</b>	
3.1 Objectives and Methods .....	F-43
3.1.1 Objectives .....	F-43
3.1.2 Method of Image Processing .....	F-43
3.2 Ground Truth Experiment .....	F-46
3.2.1 Condition and Method .....	F-46
3.2.2 Results of Experiment .....	F-46
3.3 Soil Moisture Distribution Analysis .....	F-51
3.3.1 Selection of NOAA Image for Processing.....	F-51
3.3.2 Processing of Visible/near Infrared Images .....	F-51
3.3.3 Processing of Thermal Images .....	F-52
 <b>CHAPTER 4 CONCLUDING REMARKS</b>	
4.1 LANDSAT Analysis for Topographic, Geologic and Vegetation Distribution Survey.....	F-63
4.2 NOAA Rainfall Distribution Analysis .....	F-64
4.3 NOAA Image Analysis on Soil Moisture .....	F-65

## LIST OF TABLES

		<u>Page</u>
Table F-1-1	Area Accounting of Each Basin .....	F-9
F-1-2	Area Accounting of Albedo Value .....	F-19
F-3-1	Specification of Ground Truth Experiment on Spectral Reflectance and Emissivity of Surface Soil Moisture .....	F-47
F-3-2 (1)	Daily Rainfall Amount at Conventional Gauge Sites, NOAA Image Availability and Weather Condition (Apr. 21 - May. 23, 1981).....	F-53
F-3-2 (2)	Daily Rainfall Amount at Conventional Gauge Sites, NOAA Image Availability and Weather Condition (Feb. 14 - 28 and Mar. 1 - 31, 1982).....	F-54
F-3-2 (3)	Daily Rainfall Amount at Rain Gauge Sites Installed by JICA, NOAA Image Availability and Weather Condition (Aug. 1 - 24 and Sep. 1 - 24, 1983).....	F-55
F-3-2 (4)	Daily Rainfall Amount at Gauge Sites Installed by JICA, NOAA Image Availability and Weather Condition (Dec. 1 - 31, 1984 and Jan. 1 - 31, 1985).....	F-56

## LIST OF FIGURES

		<u>Page</u>
Figure F-1-1	LANDSAT False-color Image .....	F-3
F-1-2	LANDSAT Land Classification Image .....	F-8
F-1-3	Periodic Variation of Vegetation 4-Wadi Area .....	F-17
F-1-4	Bi-Band Ratio Image .....	F-17
F-1-5	Albedo Image .....	F-20
F-1-6	Principle Component Analysis Image .....	F-20
F-1-7	Outline Map of Geology.....	F-22
F-1-8	LANDSAT Map of the Survey Area.....	F-23
F-1-9	Geological Map, Wadi-Ahin Area.....	F-26
F-1-10	Geological Map, 4-Wadi Area .....	F-27
	(From Wadi Bani Ghafir to Wadi Al-Ma'awil)	
F-2-1	Flow Chart of NOAA Data Image processing.....	F-29
F-2-2 (1)	Cloud Top Temperature Distribution Image (a) Apr.13, '83, (b) Apr. 14, '83 .....	F-31
F-2-2 (2)	" (a) Aug.9, '83, (b) Aug.14, '83.....	F-32
F-2-2 (3)	" (a) Dec.29, '84, (b) Dec.31,'84, (c) Jan.7, '85 .....	F-33
F-2-3	Flow Chart of Precipitation Distribution Analysis .....	F-37
F-2-4 (1)	Precipitation Distribution Image, Aug.10, '83 .....	F-39
F-2-4 (2)	" Dec.29, '84 .....	F-40
F-2-4 (3)	Precipitation Distribution Image, Aug.10,'83	
F-3-1	Flow chart of NOAA Image Processing for Soil Moisture Analysis .....	F-45
F-3-2	Relation between Ratio of Emissivities and Soil Water Content .....	F-48
F-3-3	Relation between Ratio of Emissivities and Moisture Condition .....	F-49
F-3-4	Relation between Ratio of Spectral Reflectance and Moisture Condition .....	F-50
F-3-5	Albedo (A1, A2) of Bands 1 and 2 of Sea Surface, Gulf of Oman, and Albedo Ratio (A1/A2) .....	F-57
F-3-6	Change of Albedo Ratio (A1/A2/SEA) Normalized by Sea before and after Rainfall in Apr. - May, 1981 at Conventional Gauge Sites .....	F-58

## CHAPTER 1 LANDSAT IMAGE ANALYSIS

### 1.1 Objectives and Methods

The study area is an extensive dry area covering about 6,000 km<sup>2</sup>. Because information on the area such as existing weather conditions or hydrology is still insufficient, there are many uncertain factors in planning a reasonable survey plan and in identifying the water balance problem with in the limited study period, scale and budget for the survey.

To eliminate such ambiguity, the remote sensing technique was complimented with conventional survey and research techniques.

The results of such remote sensing techniques were arranged in Japan simultaneously to the site survey of the project. It provides data on the extent and traces of present and past floods; watercourses and riverbed conditions for a river system; macro information, environment, vegetation and land utilization for analysis of surface layer geology; and information on topographic characteristics.

For the LANDSAT image analysis, the following data was created:

1. Color synthesized images (false color)
2. Surface covering classified images
3. Vegetation distribution time series change images
4. Albedo images
5. Analysis processing images for the topographic and geological survey

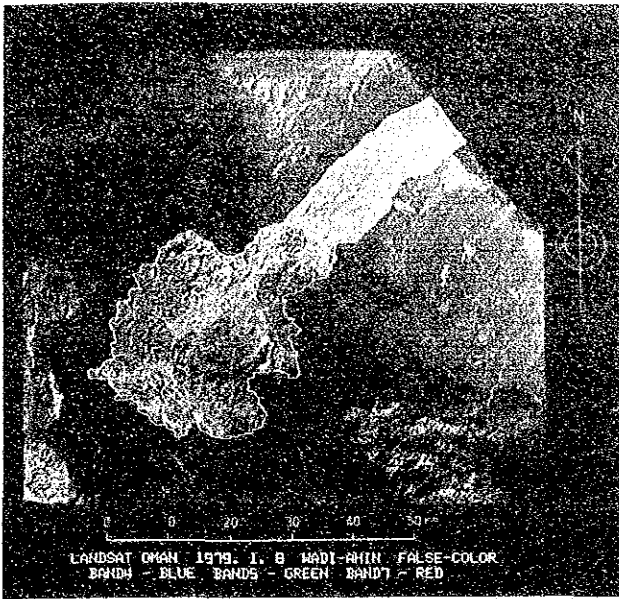
In addition, comparative computation images and birds eye view images were created.

## 1.2 Creation of Color Synthesized Images (False Color)

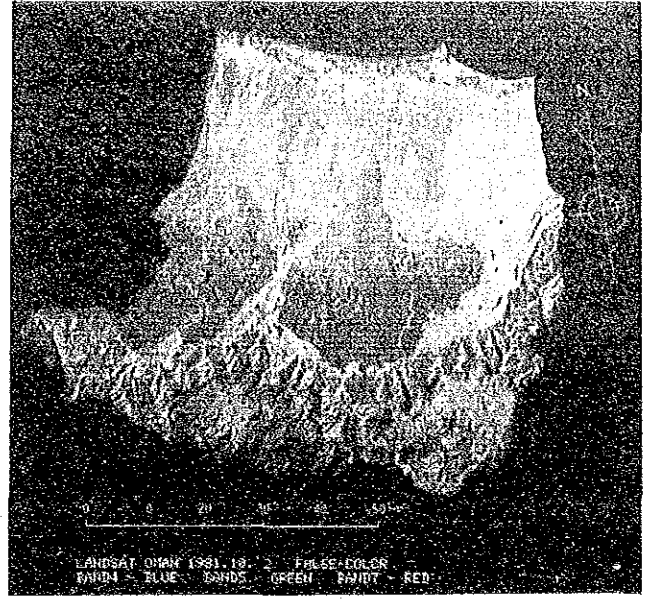
Among the LANDSAT images, the basic ones are the false color images. These images are color-synthesized to represent green of plant in red, and are very effective to grasp the distribution of vegetation. Particularly, green in the dry area such as the study area can be recognized as "controlled green."

From the false color images for four Wadi districts (Fig. F-1-1 (b)) plants are detected on the belt area oases the coast, oases along the Wadi watercourses and in the main inter-mountain districts. As also shown in the processing results described later, there is little annual change in the inter-mountain districts and the oases along the Wadi watercourses, but such changes are observed in the coastal belt areas. Annual change is also not significant for the watercourses, the riverbed conditions and the traces of Wadi floods. Less change is observed at Wadi Ahin (F-1-1 (a)) and also at the coastal belt area.

The false color images in 1984 for four Wadi areas are shown in F-1-1 (c) and are the most recent ones for the study.

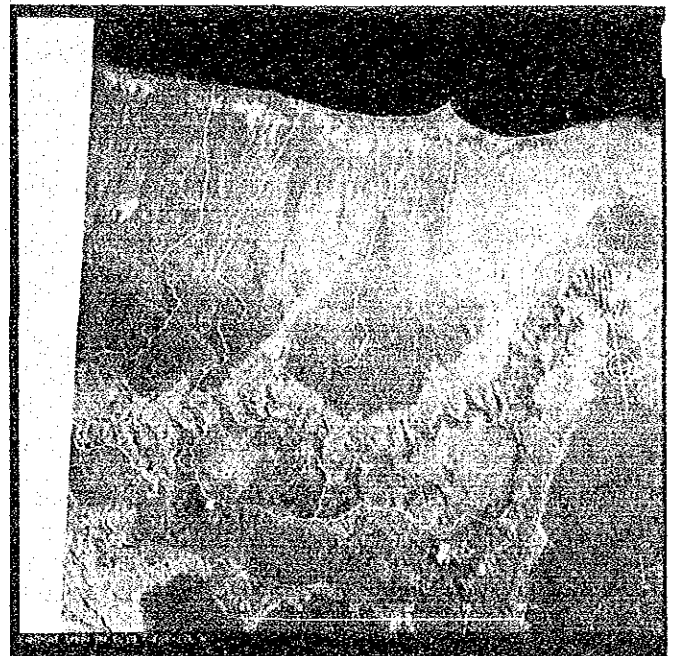


(a) Wadi Ahin Area. Jan. 8, 1979



(b) 4 Wadi Area. Oct. 2, 1981

Fig. F-1-1 LANDSAT False-color Image



(c) 4 Wadi Area Jun. 18, 1984

### 1.3 Surface Covering Classification

#### 1.3.1 Surface Covering Classified Images

##### (1) Classification processing

Generally, remote sensing information obtained from MSS is spectrum wavelength ranges over several channels.

The average energy intensity of electromagnetic waves reflected from regions occupying a certain area on the ground is obtained as MSS data for several wavelength ranges.

Therefore, identification is performed by utilizing patterns that spectrum characteristics of a specific region represent, and to indicate them.

The present classification was performed by "cluster analysis."

##### \* Cluster analysis

Cluster analysis is a technique to perform classification based on various variables, mutual distance between observation units (LANDSAT MSS data in this case) and similarity (when an analyst cannot predict groups to be classified.) Objective classification processing can be performed because there is no room for subjectivity of the analyst in how many groups data is classified or which individual data belongs to what group.

##### (2) Results of classified images (surface covering classified images)

In the present classification, the entire subject area is classified into 14 significant types.

Major items are:

1. Vegetation area (2 types)
2. Bare rock area in the mountainous district (4 types)
3. Gravel area (8 types)

In particular, vegetation is classified into the dense vegetation area (dense) and the less dense area (sparse). The vegetation area (dense) indicates an area where date palms are densely planted, while the vegetation area



(sparse) indicates an area where the date palms are sparsely planted (the coastal area, the gravel area and the mountainous district), or where there are shrubs (the mountainous district).

In addition, Wadi Ahin is classified into 16 types.

Major items are:

1. Vegetation area (2 - 3 types)
2. Bare rock area in the mountainous district (4 types)
3. Gravel area (9 - 10 types)

### 1.3.2 Features of Each Wadi from the Classified Images

#### (1) Wadi Ahin (Fig. F-1-2 (a))

This Wadi differs from the other four Wadi areas in the south in that the pivotal alluvial fan area is indistinct at the place where the Wadi riverbed flows from the foot of the mountain into the gravel field.

In addition, its gravel field differs from four Wadi areas in that it is not flat but eroded terrain. In the gravel field, the alluvial fan appears where the eroded terrain ends. There are also several Wadi riverbeds and watercourses, which form the eroded terrain. Places in the bare rock area were observed to have different spectrum characteristics, and places were observed at the deepest area of Wadi where the mountains have different structures.

#### (2) Wadi Bani Ghafir (Fig. F-1-2 (a))

The pivotal area of the alluvial fan flowing from the foot of the mountain into the gravel field is most indistinct compared with the following three Wadi. This is because the front mountain stretches for the gravel field (although it is not clear) and because the pediplane develops significantly.

#### (3) Wadi Al-Fara (Fig. F-1-2 (b))

The main riverbed is divided into three in the gravel field. Among them, the eastern most riverbed is the main riverbed that reaches to the source.

The central and west riverbeds appear to have their source at the oases at the foot of the mountain.

Bare land, which seems to be a terrace, stretches between the central and west riverbeds.

(4) Wadi Bani Kharus (Fig. F-1-2 (b))

Among the four Wadi, this one has the smallest Wadi riverbed. The main riverbed is divided into two at the top of the gravel field and the main part flows to the west of the Wadi. Both boundaries with the two adjacent Wadi constitute dunes or terraces.

(5) Wadi Al-Maawil (Fig. F-1-2 (b))

The riverbeds start near Nakhal. They distribute over wide areas and reach to the well-cultivated area in the coastal district. The basin of this Wadi has no large-scaled dune features in Wadi Bani Ghafir and its adjacent two Wadi.

(6) The front mountain and main inter-mountain district

In the front mountain, there is almost no debris soil in the valley. On the other hand, there is much debris soil in the main inter-mountain district.

According to data in 1981, it is characteristic that alpine shrubs distribute in substantial density in the main inter-mountain district, whereas little is observed in the front mountain.

### 1.3.3 Result of Classification of Dense and Sparse Vegetation

(1) Coastal district

In the coastal district, areas classified as "dense" have a lot of vegetation while areas classified as "sparse" have only a little.

It appears that the planted density of date palms is low, and that the ground under the trees is sometimes utilized as farm land.

- (2) Upstream area of the gravel field, the front mountain and the main inter-mountain district

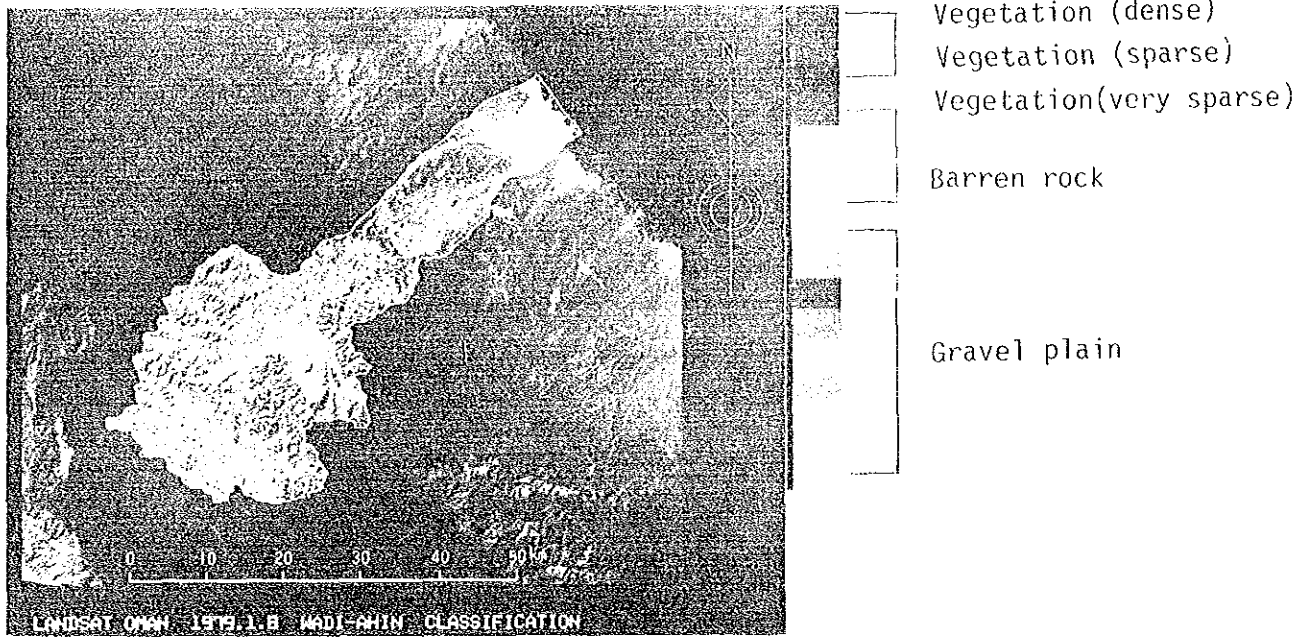
These districts contrast the coastal district, and areas classified as "dense" are predominant.

It appears that the vegetation density of date palms planted in this district is high, and that the number of developed branches and average height of the trees differ from those in the coastal district.

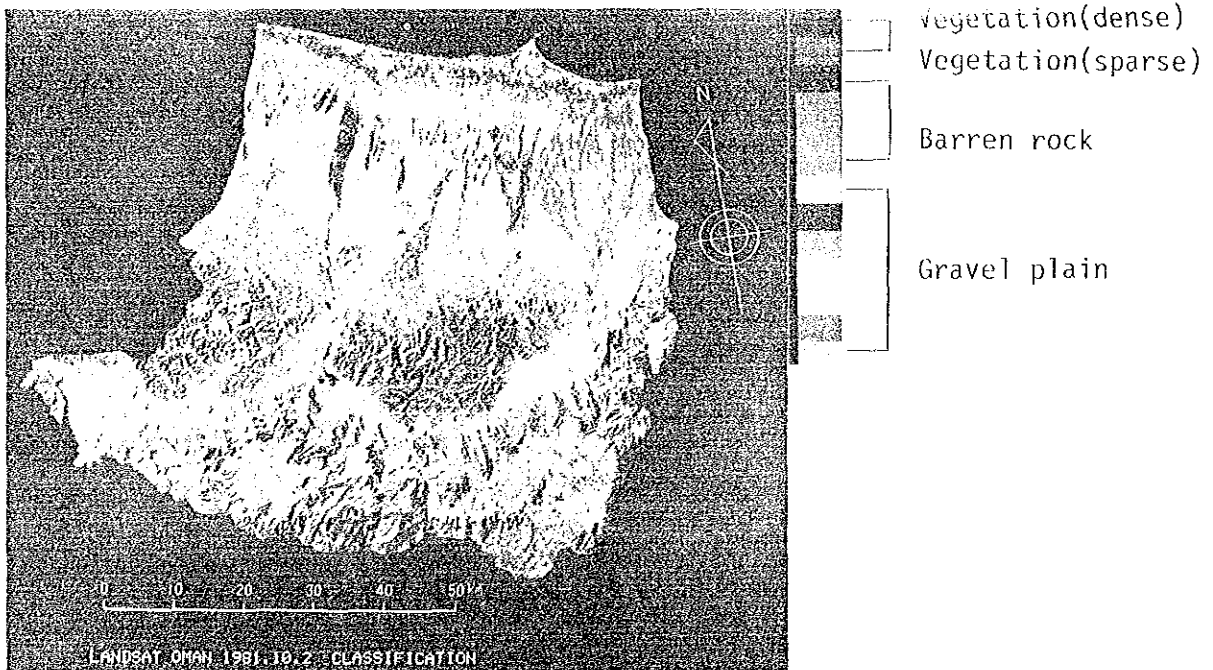
- (3) Around divides at the deepest area of each Wadi

These areas are mostly classified as "sparse". The vegetation appears to be alpine shrubs as indicated by the results of the survey in 1982.

Fig. F-1-2 LANDSAT Land Classification Image



(A) Wadi Ahin Area, Jan. 8, 1979



(B) 4 Wadi Area, Oct. 2, 1981

### 1.3.4 Area Accounting

The following tables shows the occupied area (unit: ha) by major item, and figures in the parenthesis indicate percentage to the total area of each basin.

Table F-1-1(1) Area Accounting of Each Basin (1/3)

(1) Wadi Ahin

Total area: 1,127.54 km<sup>2</sup> (112,754 ha)

Major item	Year	
	1972 October	1979 January
Vegetation (dense)	220 ha (0.20%)	389 ha (0.34%)
Vegetation (sparse)	3,556 (3.15)	4,859 (4.31)
Bare rock district	33,963 (30.12)	39,595 (35.12)
Gravel field	75,014 (66.53)	67,912 (60.23)

Table F-1-1 (2) Area Accounting of Each Basin (2/3)

(2) Wadi Bani Ghafir

Total area 951.90 km<sup>2</sup> ( 95,190 ha )

main item \ year	1972	1978	1981
	OCT. (ha)	DEC. (ha)	OCT. (ha)
Vegetation (dense)	220 ( 0.23)	260 ( 0.27)	456 ( 0.48)
Vegetation (sparse)	1,668 ( 1.75)	3,750 ( 3.94)	6,739 ( 7.08)
Barren rock	43,813 (46.03)	41,277 (43.36)	40,775 (42.84)
Gravel plain	49,489 (51.99)	49,903 (52.42)	47,220 (49.61)

(3) Wadi Fará

Total area 1,546.75 km<sup>2</sup> ( 154,675 ha )

main item \ year	1972	1978	1981
	OCT. (ha)	DEC. (ha)	OCT. (ha)
Vegetation (dense)	505 ( 0.33)	630 ( 0.41)	687 ( 0.44)
Vegetation (sparse)	1,258 ( 0.81)	2,642 ( 1.71)	5,807 ( 3.75)
Barren rock	54,712 (35.37)	48,666 (31.46)	52,165 (33.73)
Gravel plain	98,200 (63.49)	102,737 (66.42)	96,016 (62.08)

(4) Wadi Bani Kharus

Total area 1,292.32 km<sup>2</sup> ( 129,232 ha )

main item \ year	1972	1978	1981
	OCT. (ha)	DEC. (ha)	OCT. (ha)
Vegetation (dense)	184 ( 0.14)	303 ( 0.23)	457 ( 0.35)
Vegetation (sparse)	2,513 ( 1.94)	4,679 ( 3.62)	10,557 ( 8.17)
Barren rock	50,298 (38.92)	51,967 (40.21)	50,834 (39.34)
Gravel plain	76,237 (58.99)	72,283 (55.93)	67,384 (52.14)

Table F-1-1(3) Area Accounting of Each Basin (3/3)

(5) Wadi Ma'awil

Total area 1,029.77 km<sup>2</sup> ( 102,977 ha )

main item \ year	1972	1978	1981
	OCT. (ha)	DEC. (ha)	OCT. (ha)
Vegetation (dense)	246 ( 0.24)	351 ( 0.34)	456 ( 0.44)
Vegetation (sparse)	918 ( 0.89)	1,636 ( 1.59)	5,124 ( 4.98)
Barren rock	29,233 (28.39)	29,432 (28.58)	27,723 (26.92)
Gravel plain	72,580 (70.46)	71,558 (69.49)	69,674 (67.66)

(6) 4-Wadi (total)

Total area 4,820.74 km<sup>2</sup> ( 482,074 ha )

main item \ year	1972	1978	1981
	OCT. (ha)	DEC. (ha)	OCT. (ha)
Vegetation (dense)	1,155 ( 0.24)	1,544 ( 0.32)	2,056 ( 0.43)
Vegetation (sparse)	6,357 ( 1.32)	12,707 ( 2.64)	28,227 ( 5.87)
Barren rock	178,056 (36.94)	171,342 (35.54)	171,497 (35.57)
Gravel plain	296,506 (61.51)	296,481 (61.50)	280,294 (58.14)

### 1.3.5 Correspondence between the Classified Images and Air Photos

Air photos of 1:30,000 scale shot in 1981 were compared with the LANDSAT classified images the same year.

The results of correspondence are as follows.

#### (1) Coastal belt district

In this district, there is vegetation (sparse) among vegetation (dense). The vegetation (dense) is farms, while the vegetation (sparse) represents farms, palms or scattered trees. Many farms around the vegetation (sparse) are not recognizable by the remote sensing. It is revealed from the air photos that the regions of plantation is so sparse that they cannot be identified as the vegetation. Such farms are classified as the "gravel field VI" in most cases, but, in some places, they are classified as the "gravel field V or VI."

Colonies are scattered in or around the "vegetation." The coastal colonies, which appear to be fishing villages, show the spectrum characteristics similar to that of the gravel field.

On the air photos, shrubs with considerable density and extent are observed in the gravel fields by road near Billar of Wadi Bani Kharus. However, these areas are not "controlled green," and they are not identified as vegetation on the classified images.

This reveals that all of those classified as the vegetation in this district are the "controlled green."

#### (2) Gravel field

The gravel fields are classified into several types because the spectrum characteristics differ depending whether the watercourses are new or old. Although the surface terrain cannot be identified from the remote sensing data, the air photos allow observation of such details as wind-wrought patterns on the dunes or monadnocks.

According to the air photos, all the vegetation (dense) in the gravel field are palms, the vegetation (sparse) is farms. Only a section of farms and colonies are classified as the "gravel field VI." In addition, the shrubs



scattered in the surrounding watercourses are not recognized as the vegetation.

(3) The front mountain

The vegetation (sparse) here is distributed along the watercourses. According to the air photos, they are all palms, "controlled green." Although shrubs are dense in the surrounding areas, they are not recognized as vegetation in the remote sensing data.

(4) Al-Rustaq, Al-Awabi and Nakhal

The vegetation (dense) in these areas are palms according to the air photos. Those classified as the vegetation (sparse) are productive farms. Only a section of farms and colonies are classified as "gravel field VI or VII."

(5) The main inter-mountain district

The vegetation (dense) in the watercourses in the main intermountain district are all palms according to the air photos with the vegetation (sparse) around them being productive farms. Only a section of farms and colonies are classified as the "gravel field VI or VII."

The independent vegetation (sparse) distributed away from the vegetation (dense) are small-scale palm colonies, terraced farms or shrubs. In some cases, the shrubs near the divides may be classified as the vegetation (sparse) because they differ from those in the gravel fields in that they are of larger scale and higher density.

## 1.4 Vegetation Distribution

### 1.4.1 Vegetation Distribution Periodic Series Change Images

The time series change pattern diagram (images) indicate development and shrinkage in three periods from the vegetation among the classification items. (Fig. F-1-3)

Evaluation criteria for such change patterns are as follows:

Existence of Vegetation			
Legend of Classification	Year		
	1972	1978	1981
Y-Y-Y	Existence	Existence	Existence
N-Y-Y	Non-existence	Existence	Existence
N-N-Y	Non-existence	Non-existence	Existence
Y-Y-N	Existence	Existence	Non-existence
Y-N-N	Existence	Non-existence	Non-existence

The changes for four Wadi can be seen by comparing the vegetation (dense and sparse) and the vegetation (dense) on the two types of time series change patterns diagrams (images). Fig. F-1-3 shows the vegetation (dense and sparse).

### 1.4.2 Features of the Periodic Series Change Pattern Diagrams

#### (1) Coastal district

Of the three periods, only in 1978 do areas with vegetation exist prominently near the coast. On the other hand, areas not observed in the previous two periods but appearing in 1981 are significant at areas from the cultivated belt to the gravel fields.

This indicates that areas with vegetation (cultivated fields) at the coast are expanding to the gravel fields in the periodic series. Possible causes of this expansion are weather, saltwater intrusion and increase of irrigation facilities.

Isobath at 10 m of the "hydro-isobath" obtained by the survey in 1982 corresponds well to the distribution of cultivated farms.

There are a few areas that existed in the previous two periods but disappeared in 1981.

(2) Gravel field

In 1981, existence of vegetation was observed along main riverbeds of each Wadi, particularly in Wadi Bani Kharus.

(3) The foot of the mountain and the front mountain

Although there are unchanged and changed areas in the periodic series for oases areas at the foot of the mountain, unchanged ones are prominent in general. Thus, it appears that even oases repeat development and contraction as a whole.

Dunes crossing Wadi Al-Fara and Wadi Bani Kharus showed vegetation in 1976 although it was sparse. There are a few areas over the foot of the mountain that disappeared in 1981.

(4) Main intermountain district

In Rustaq, Al-Awabi and Nakhal, unchanged areas are prominent with a few changed areas around them. Some well-cultivated fields which exist along both side of the Wadi in the inter-mountain district show changes in the periodic series, indicating that they repeatedly develop and contract as a whole.

Developing and contracting vegetation belts distribute to a considerable extent near the divides at the deepest area of each Wadi and near the peaks of mountains surrounding basins. A considerable number of areas in all three periods are observed near the divide at the deepest area of Wadi Al-Ma'awil. It appears that these areas have considerable rainfall throughout a year.

Throughout the three periods, little vegetation was observed in the Al-Ghubrah basin in the main inter-mountain district.

### 1.4.3 By-band Ratio Images

While the vegetation areas are divided into two, "dense" and "sparse" in the classified images, no clear difference in the type of vegetative cover exists in these two classification. It is generally known that, when by-band computation is conducted between Band 7 and Band 4, or between Band 7 and Band 5, the vegetative cover ratio (amount of plants) is emphasized. Band 7 is a band covering near infrared range that has a high reflection factor. On the other hand, Bands 4 and 5 represent the intensity of reflection factor against the ground surface (bare ground).

By-band computation, the following results are obtained:

(Area with many plants)	(Area with few plants)
$\frac{\text{Band 7}}{\text{Band 4 or 5}}$ .... high	$\frac{\text{Band 7}}{\text{Band 4 or 5}}$ .... low
..... low	..... high

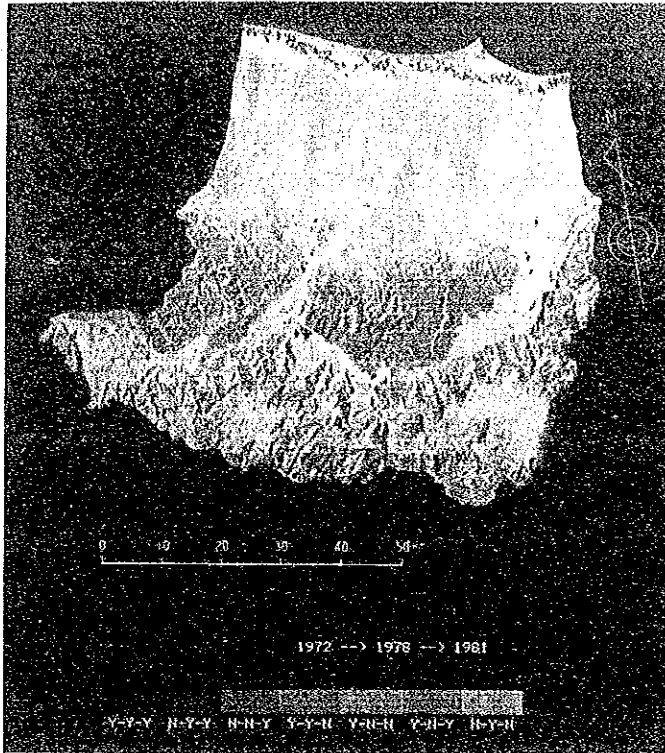
this emphasizes the vegetative cover ratio.

Fig. F-1-4 (b) shows an image that assigns colors for the results of computation on Band 7/Band 4 for the four Wadi. It indicates that the number of plants becomes higher close to the warm color (red).

From Fig. F-1-4 (b) it is found that the oases (such as Rustaq) have a very high vegetative cover ratio, and that shrubs on the well-cultivated farms at the coastal district and the mountainous district distribute extensively at higher levels above the sea. There is little vegetation in the gravel fields or the front mountains.

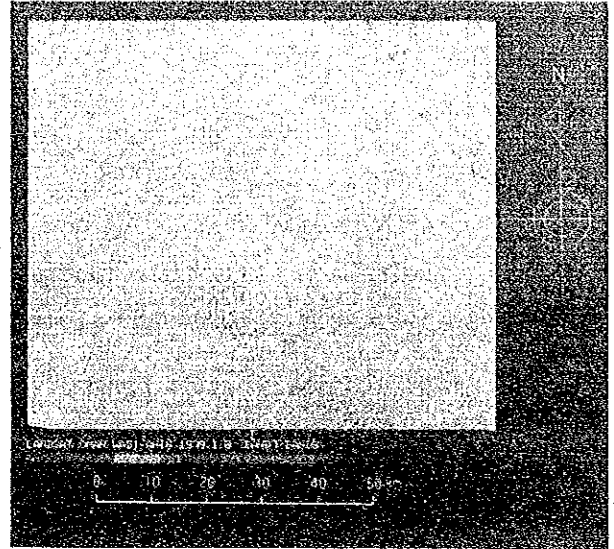
Such difference in the number of plants reflects water environment, terrain and geology of each district, and can be utilized as basic data for assessing the water balance.

Fig. F-1-3 Periodic Variation of Vegetation 4-Wadi Area (1972, 1978, 1981)

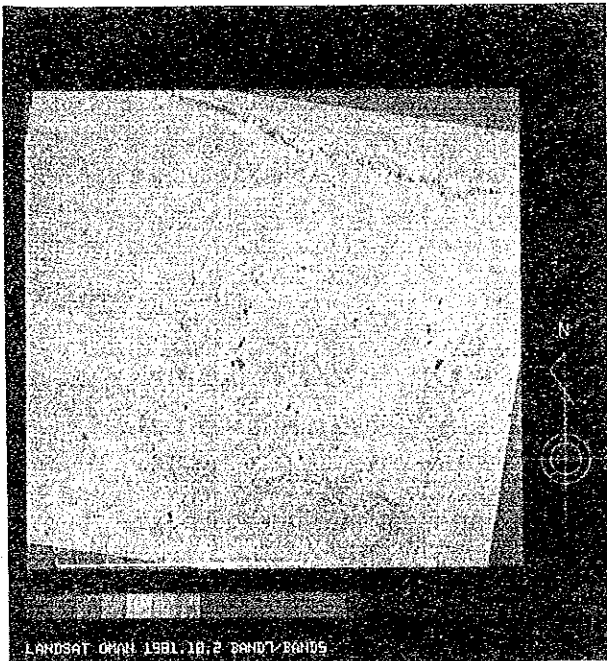


4 Wadi Area (1972,1978,1981)

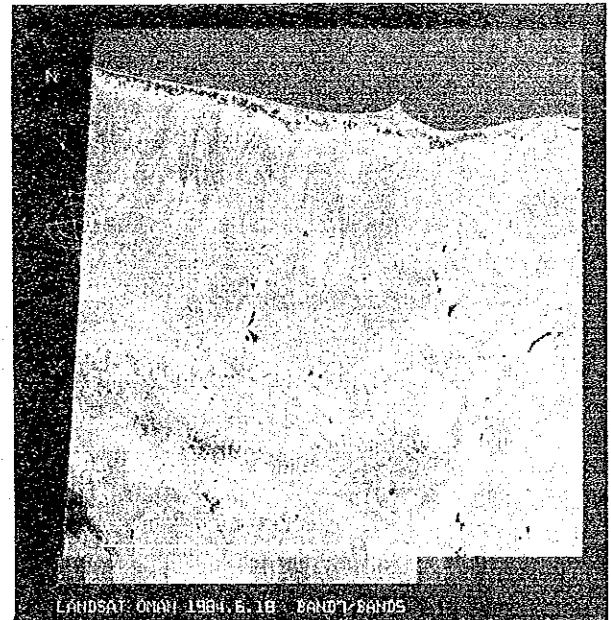
Fig. F-1-4 Bi-Band Ratio Image



(a) Wadi Ahin Area. Jan. 8, 1979



(b) 4 Wadi Area. Oct. 2, 1981



(c) 4 Wadi Area. Jun. 18, 1984

## 1.5 Albedo Images

### 1.5.1 Albedo Images

Albedo distribution images for five scenes covering four Wadi and Wadi Ahin were generated by calculating the amount of albedo against incident light of the wavelength range for four bands of the LANDSAT (0.5 - 1.1  $\mu\text{m}$ ). There is little difference between these calculated albedo values and the albedo values as obtained at wavelength of 0.3 - 3.0  $\mu\text{m}$ .

Quadrature was conducted from the albedo distribution images for each percentage.

Photos-10 and 11 show the albedo images for four Wadi in 1981 and Wadi Ahin in 1979, respectively.

The albedo images show the distribution of reflection factors for short wavelength (0.5 - 1.1  $\mu\text{m}$ ) on the ground surface. Since the reflection factors on the ground surface have close relation with the radiated heat balance of that area, it very much shows the heat distribution on the ground. It also provides information differing from those of the false color and the classified images.

### 1.5.2 Albedo Image - Quadrature

#### (1) Wadi Ahin (Fig. F-1-5 (a))

Contrary to the four other Wadi, this wadi has low reflection factor on the river course and areas exceeding 30% are observed at the coastal district.

#### (2) Four Wadi (Fig. F-1-5 (b))

Areas exceeding the reflection factor of 35% exist at the well-cultivated farms along the coast and neat Nakhl, which are classified as silt areas. The river course of Wadi Al-Maawil has higher reflection factor than those for other three Wadi, so that it can be identified from the albedo image. It appears that the deposit on the river course is much whiter than other three Wadi, or there was frequent flood. The river courses of the other three Wadi also have some unique features.

Table F-1-2 Area Accounting of Albedo Value

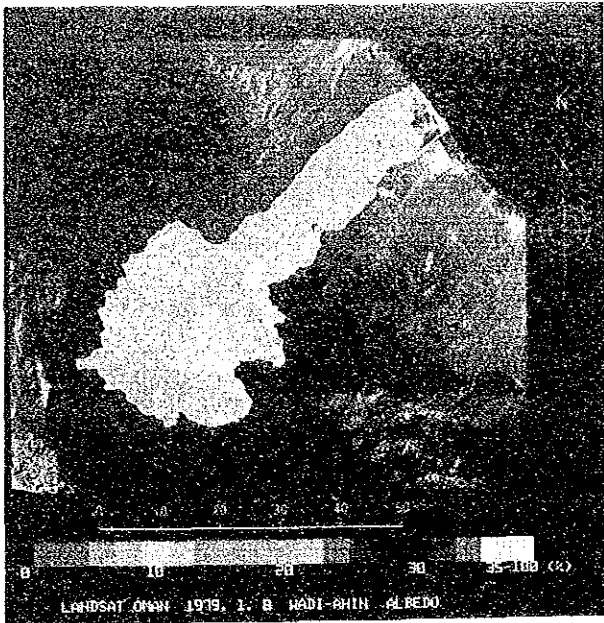
(1) Wadi Ahin Area

Data	Area per albedo (ha)	
	Nov. 28, '72	Jan. 8, '79
Albedo (%)		
0	-	-
1 - 2	-	-
3 - 4	482	115
5 - 6	3,144	1,663
7 - 8	5,765	4,993
9 - 10	8,200	7,323
11 - 12	10,955	11,062
13 - 14	21,237	15,387
15 - 16	27,298	23,557
17 - 18	20,257	22,452
19 - 20	8,769	16,708
21 - 22	3,717	6,492
23 - 24	1,459	1,780
25 - 26	661	833
27 - 28	437	287
29 - 30	219	85
31 - 32	112	17
33 - 34	34	-
35 - 100	8	-

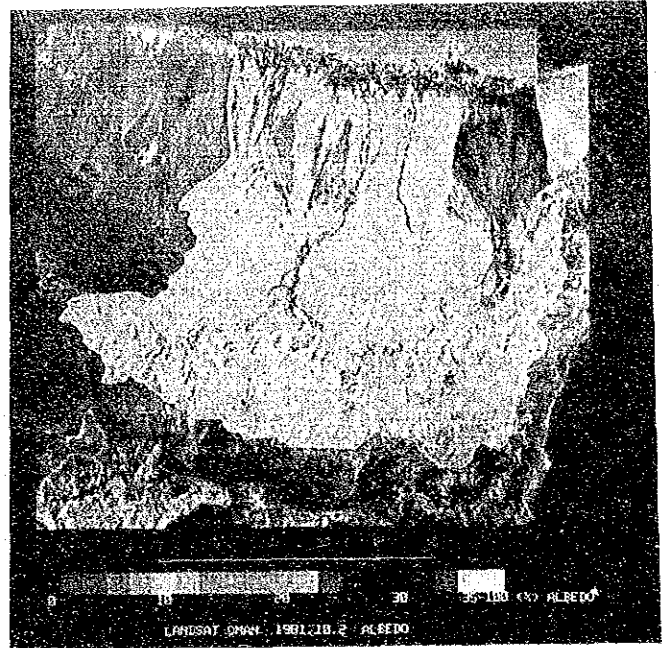
(2) 4 Wadi Area

Data	Area per albedo (ha)		
	Nov. 28, '72	Jan. 8, '79	Oct. 2, '81
Albedo (%)			
0	-	-	-
1 - 2	299	-	-
3 - 4	1,864	3,697	598
5 - 6	6,013	14,490	4,707
7 - 8	7,866	16,912	4,346
9 - 10	17,843	24,808	9,255
11 - 12	30,858	38,062	20,357
13 - 14	45,769	47,499	36,426
15 - 16	54,297	60,902	53,496
17 - 18	53,267	107,300	65,533
19 - 20	92,799	97,391	82,845
21 - 22	83,169	44,770	86,164
23 - 24	44,786	15,659	60,801
25 - 26	22,281	6,153	32,801
27 - 28	10,460	2,808	13,780
29 - 30	4,632	1,283	5,410
31 - 32	2,566	509	2,640
33 - 34	1,647	113	1,560
35 - 100	1,658	20	1,355

Fig. F-1-5 Albedo Image

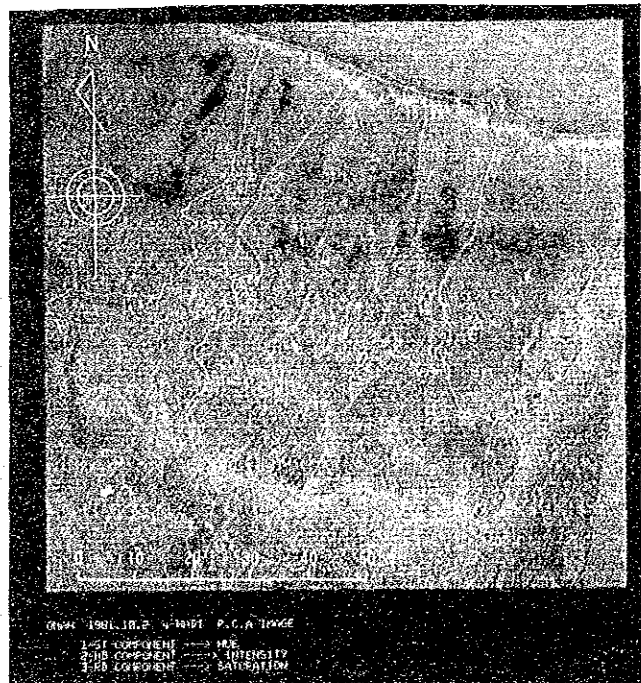


(a) Wadi Ahin Area. Jan. 8, 1979



(b) 4 Wadi Area. Oct. 2, 1981

Fig. F-1-6 Principle Component Analysis Image



4 Wadi Area. Oct. 2, 1981



## 1.6 Analysis Image Processing for the Topographic and Geological Survey

### 1.6.1 Result of Analysis Image

Fig. F-1-7 and F-1-8 show a LANDSAT map overlaid with the results of analysis.

### 1.6.2 Principle Component Analysis Images

Because the survey area lies in a dry zone, the ground surface is exposed and this allows relatively easy analysis of the topographic and geological structure. Keys for such analysis are these three elements of color tones, patterns and textures appearing on the images. Although basic images for the analysis are the color synthesized images, technique emphasizing images analysis may be effective in some cases to increase amount of information for the analyst.

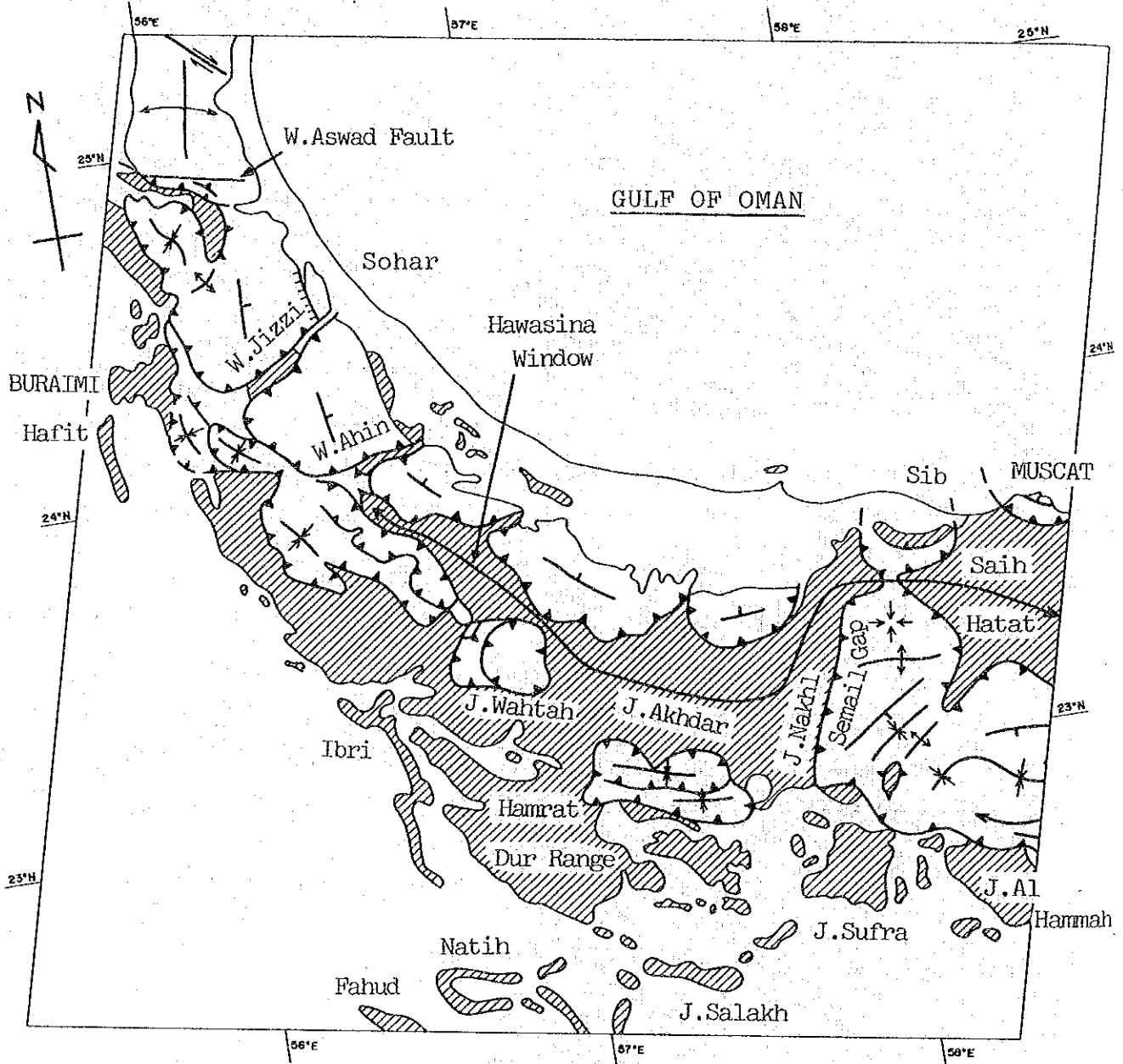
The image analysis techniques include: (1) edge emphasis, (2) computation process and (3) statistic technique. (1) is mainly effective for emphasizing texture, (2) is for emphasizing objects.

This analysis was prepared by analyzing main components with statistic techniques (3).

The principle component analysis analyzes the main components as follows: utilizing LANDSAT data in four bands, finding factors for calculating the values of first to third components, and determining scores for each of the components from these factors. The output is synthesized by assigning a hue most sensitive to the human vision to the first component, intensity of brightness of the hue to the second component and its chroma to the third component. Fig. F-1-6 shows the results (principle component analysis image).

Calculation reveals that the difference of the first component or the hue represents intensity of reflection factors of the ground surface and that of the second component or the brightness the difference of vegetative cover ratio.

Fig. F-1-7 Outline Map of Geology



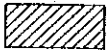

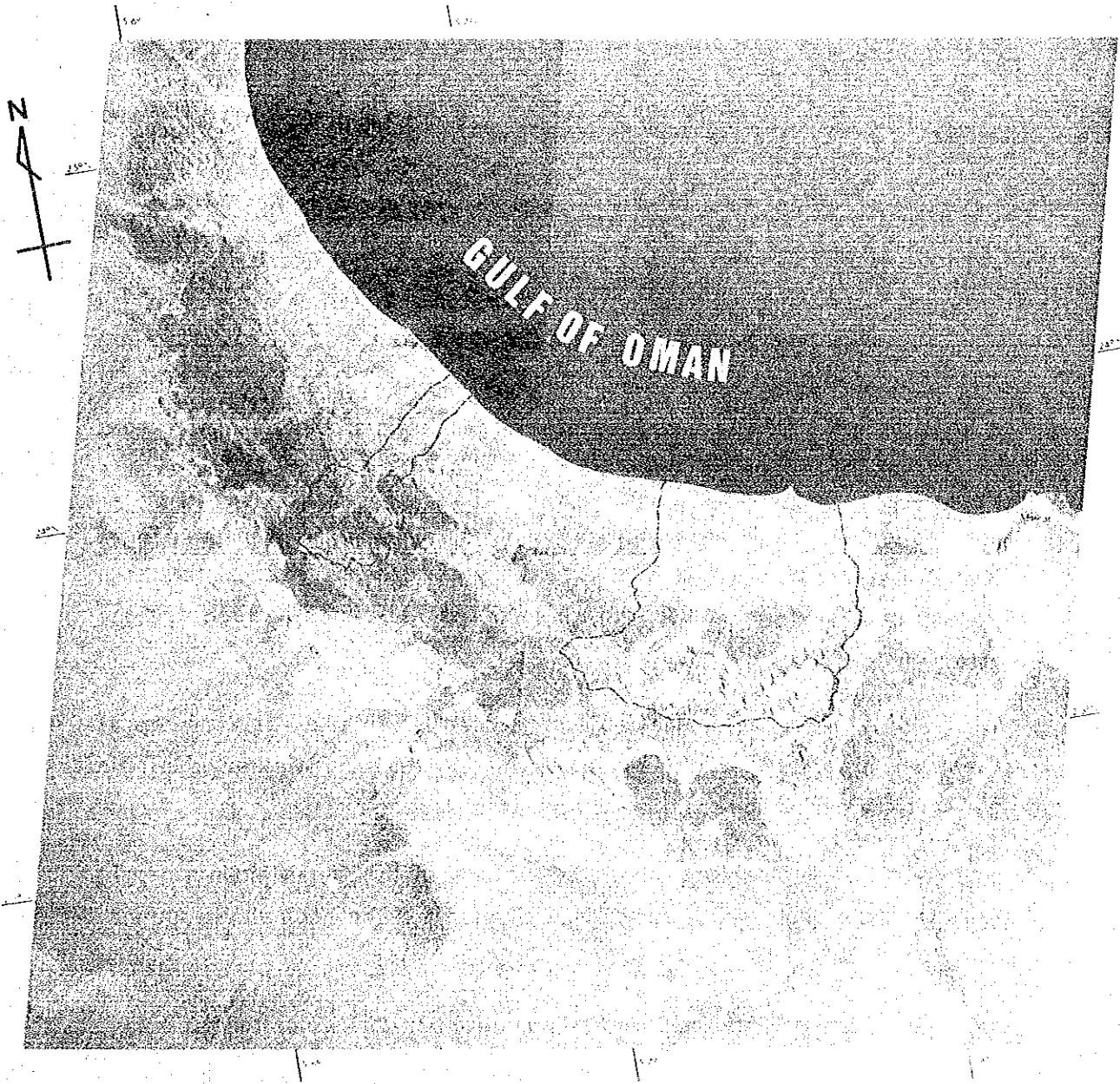
-  Autochthonous, Tertiary, Hawasina & Sumeini
-  Semail Nappe

Fig. F-1-8 LANDSAT Map of the Survey Area



The objects to be analyzed by utilizing the color synthesized image or the principle component analysis image obtained above are mainly geology and lineament.

Image information is difficult to recognize on the ground or the air photos because of their small scale, but it does provides macro information for configuration and continuity of the entire study area.

Fig. F-1-9 and F-1-10 show the results of analysis for the topographic and geological survey.

### 1.6.3 Features of the Study Area Based on Analysis Results

Legends in the figures are those of the existing materials (geological map) combined with the analysis chart from the LANDSAT data. The directional distribution of lineament for each district is shown in the form of a rose chart secondary information.

The surveyed area lies near the center of the Oman Mountains and faces the Batinah Coast. The foundation of the Oman Mountains consists of the Pre-Permian system and the Permian-Cretaceous system, which are the main constituent of the mountains.

The mountains has large-scale overturned structure caused in the upper Cretaceous period, and formed and deformed by the orogenic movements in the Tertiary period to provide a complicated structure.

Some of the complicated geological structures in the Oman Mountains can be detected by comparing the LANDSAT map and the geological summary map.

- 1 The area distributed with semail ophiolite has dark color tone.
- 2 The area where the Tertiary layer, the Hawasina layer and the Sueini layer distribute is represented in dark gray.

Specific geological features are:

- 1 The Hawasina window is clearly identified.
- 2 Semail ophiolite is clearly bounded, which is indicated as an overturned fault in the geological map.
- 3 In the Akhdar Mountain, a large-scaled anticlinal axis bent in the east-west direction. The anticlinal ridge is eroded to continuous basins of various sizes including Ghubrah Bow.
- 4 Semail gap forms a clear and linear valley NNE-SSW.
- 5 Many geologic-lineaments are observed and correspond well to the faults in the geological map. Generally, the main faults (or geologic-lineaments) coincide with the extensions of the Oman Mountains, direct to east-west at the eastern area and changing to north-south in the northeastern area.

Features of the lowland are:

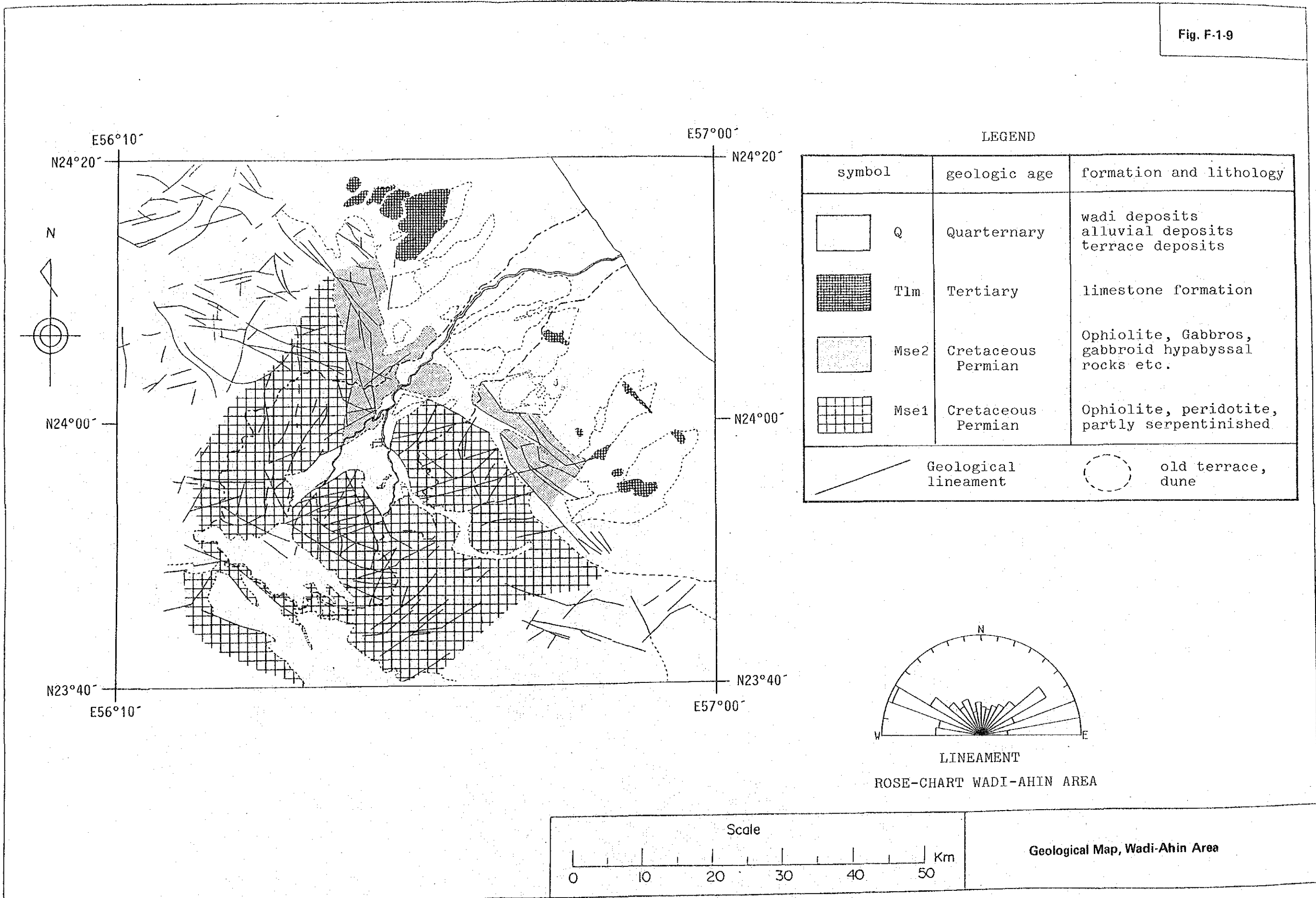
- 1 Distribution of inland deserts and detailed distribution of Wadi.
- 2 On the coast of the Oman Bay many extensive alluvial fans are formed by sand and soil flowing from the Oman Mountains.
- 3 Narrow coastal plain is formed along the coast and utilized for farms.

The above-mentioned features are part of the large-scaled pattern, but the LANDSAT images contain more detailed information of topography and geology.

The layers of Pre-Permian or Permian period in the Akhdar Mountains can be further sub-divided by darkness and color tones which correspond to the different rocks. In addition, there are several differences in the distribution of semail ophiolite.

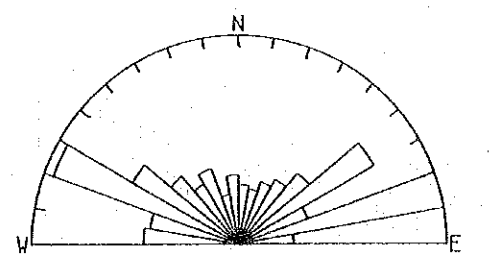
In the alluvial fans, there are clear differences in darkness, which may correspond to the time when they were formed, the distribution of dunes, etc.

Fig. F-1-9

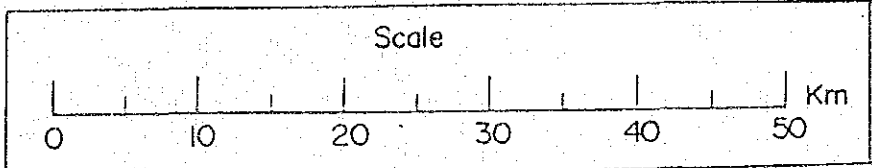


LEGEND

symbol	geologic age	formation and lithology
Q	Quarternary	wadi deposits alluvial deposits terrace deposits
Tlm	Tertiary	limestone formation
Mse2	Cretaceous Permian	Ophiolite, Gabbros, gabbroid hypabyssal rocks etc.
Mse1	Cretaceous Permian	Ophiolite, peridotite, partly serpentinitised
	Geological lineament	
		old terrace, dune

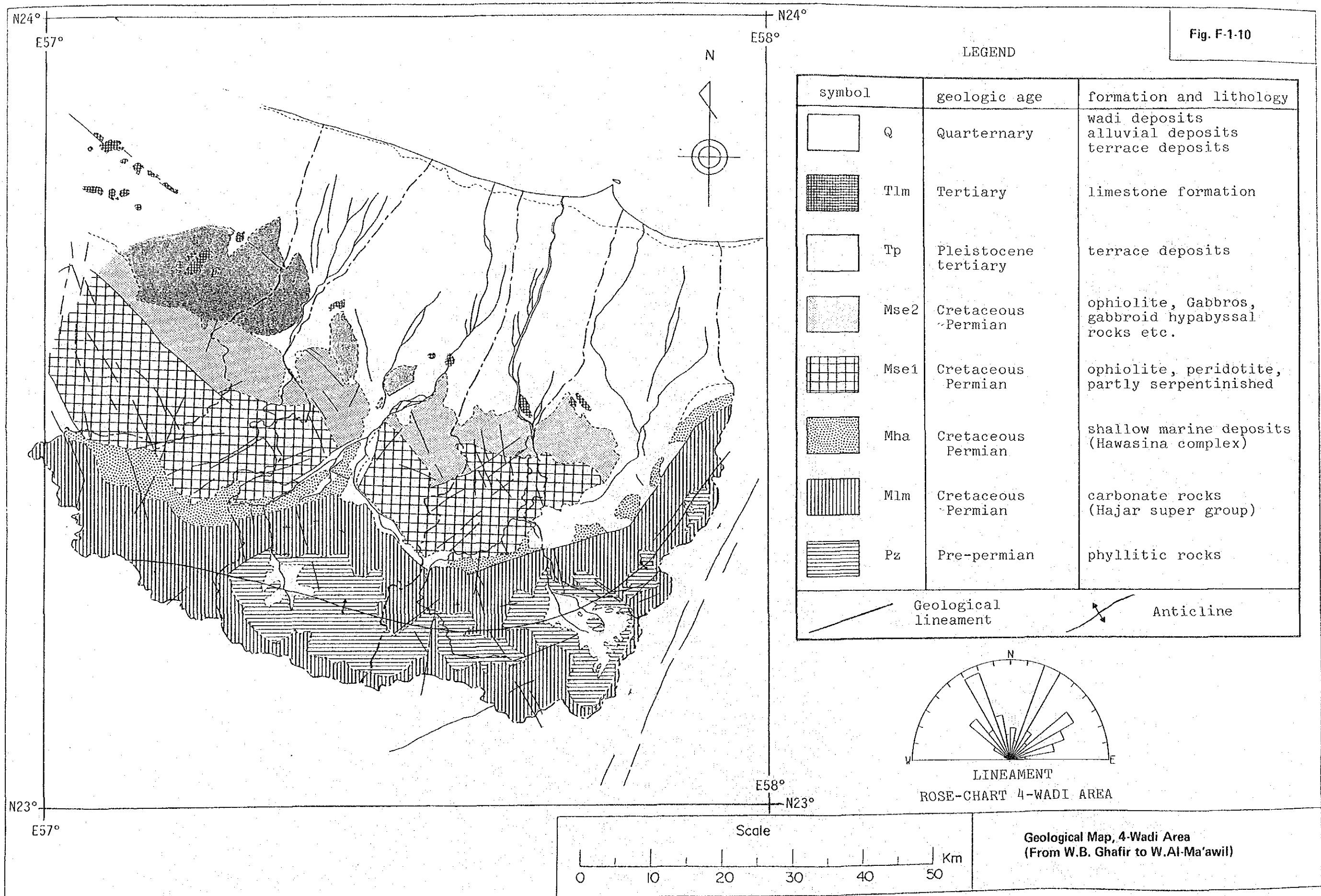


LINEAMENT  
ROSE-CHART WADI-AHIN AREA



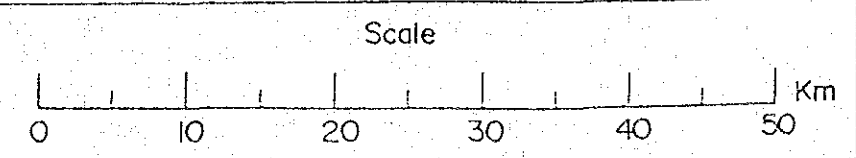
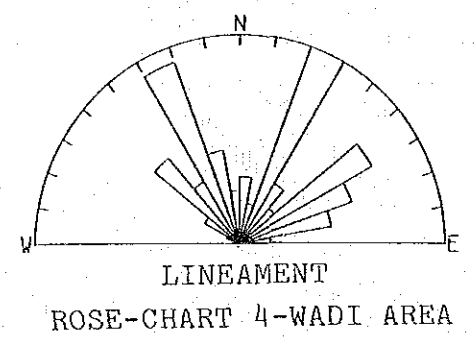
Geological Map, Wadi-Ahin Area

Fig. F-1-10



LEGEND

symbol	geologic age	formation and lithology
Q	Quarternary	wadi deposits alluvial deposits terrace deposits
T1m	Tertiary	limestone formation
Tp	Pleistocene tertiary	terrace deposits
Mse2	Cretaceous -Permian	ophiolite, Gabbros, gabbroid hypabyssal rocks etc.
Mse1	Cretaceous Permian	ophiolite, peridotite, partly serpentinished
Mha	Cretaceous Permian	shallow marine deposits (Hawasina complex)
M1m	Cretaceous -Permian	carbonate rocks (Hajar super group)
Pz	Pre-permian	phyllitic rocks
	Geological lineament	
	Anticline	



Geological Map, 4-Wadi Area  
(From W.B. Ghafir to W. Al-Ma'awil)





## CHAPTER 2 NOAA RAINFALL DISTRIBUTION ANALYSIS

### 2.1 Objectives and Methods

It is necessary to assess rainfall amount in the study area in order to determine water balance, which is one of the objectives of the survey. Therefore, 28 observation sites for the rainfall amount were provided in the study area. The observation started in August, 1983.

In order to determine the extent of an area covered by the data obtained from each observation point, the study utilizes the cloud images (brightness-temperature images) of NOAA to assess the rainfall amount by reasonably extending the rainfall data from the ground observation points to a plane.

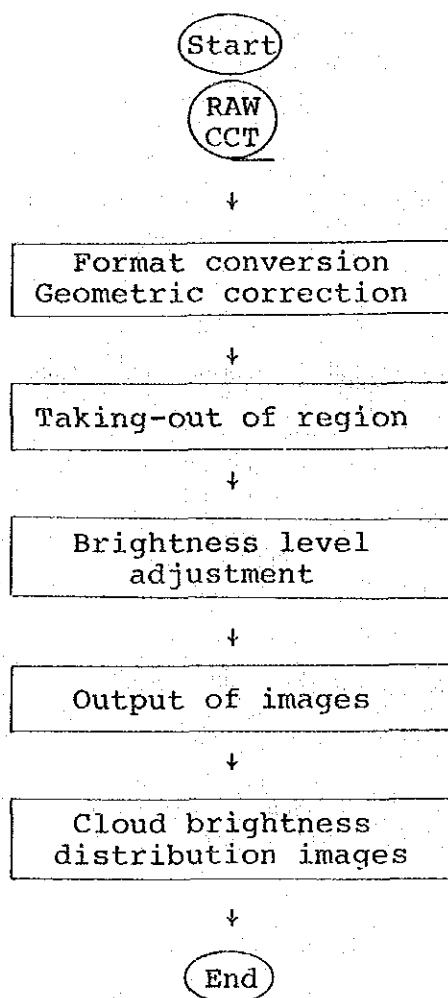
In the rainfall distribution analysis, the rainfall amount distribution is estimated based on upper altitude weather data of Seeb Airport in addition to the cloud image information of NOAA and the rainfall data at the ground observation sites (location, height, amount).

Seven NOAA images were collected for the rainfall distribution analysis taken on August 10, 1984 and December 29, 1984 when rainfall was also observed on the ground, as well as on April 13 and 14, 1983, August 9, 1983, December 31, 1984 and January 7, 1985 when rainfall was neither observed on the ground nor at some of the 28 rain gauges.

## 2.2 Image Processing

NOAA digital data was used for the rainfall analysis. The digital data acquired is output as images after the format conversion, level adjustment and geometrical correction. The output procedure follows the flow shown in Figure F-2-1.

Fig. F-2-1 Flow Chart of NOAA Data Image Processing

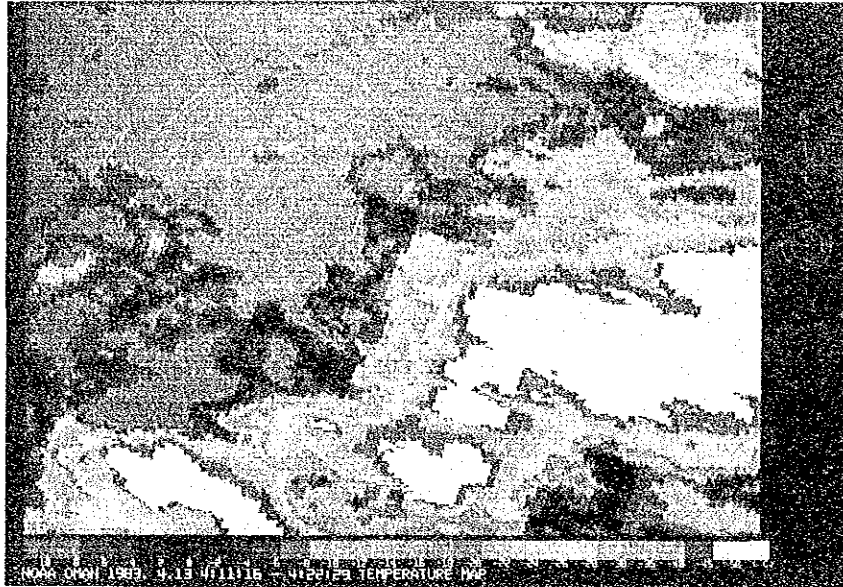


The UTM projection chart is used for the geometric correction, and is adjusted so that the brightness of cloud does not saturate the images. (Fig. F-2-2 (1) -(3))

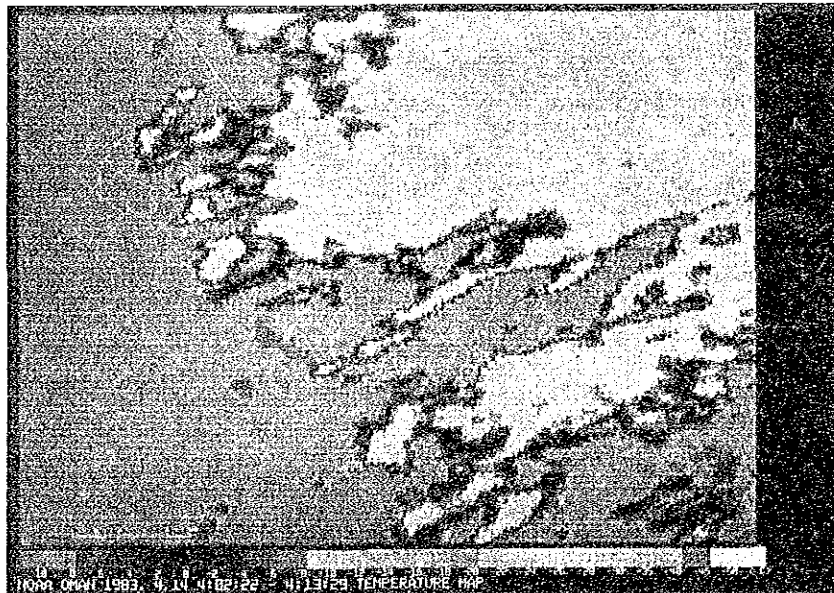
The cloud brightness (temperature of the peak of the cloud) thus obtained represents thickness of the cloud, and is believed to bear a close relationship to the rainfall. It is, however, required to consider the

altitude where the cloud develops and the type of cloud (such as altostratus, middle cloud or low cloud). However, only a limited number of techniques could be used in this analysis considering the extent of 6,000 km<sup>2</sup>, the rainfall in the dry zone and limited weather information.

Fig. F-2-2 (1) Cloud Top Temperature Distribution Image (1/3)



(a) Apr. 13, 1983

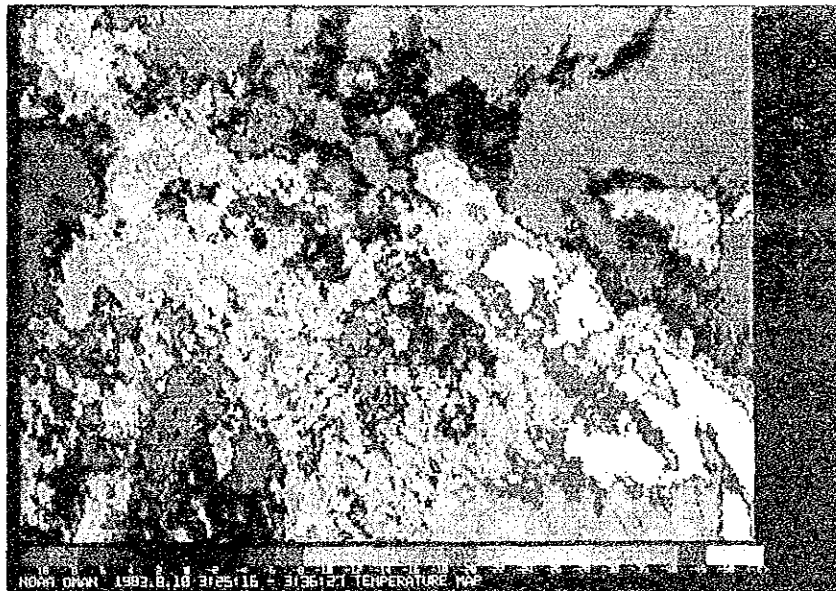


(b) Apr. 14, 1983

Fig. F-2-2(2) Cloud Top Temperature Distribution Image (2/3)

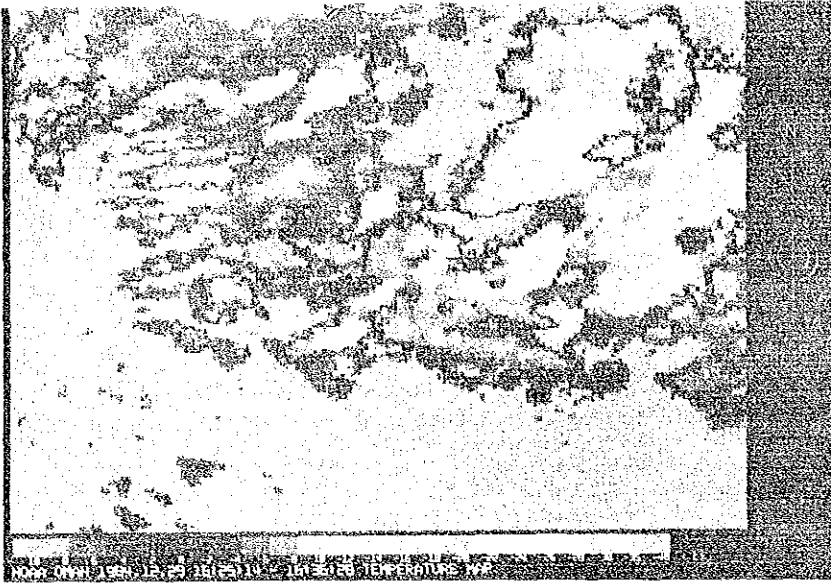


(a) Aug. 9, 1983



(b) Aug. 10, 1983

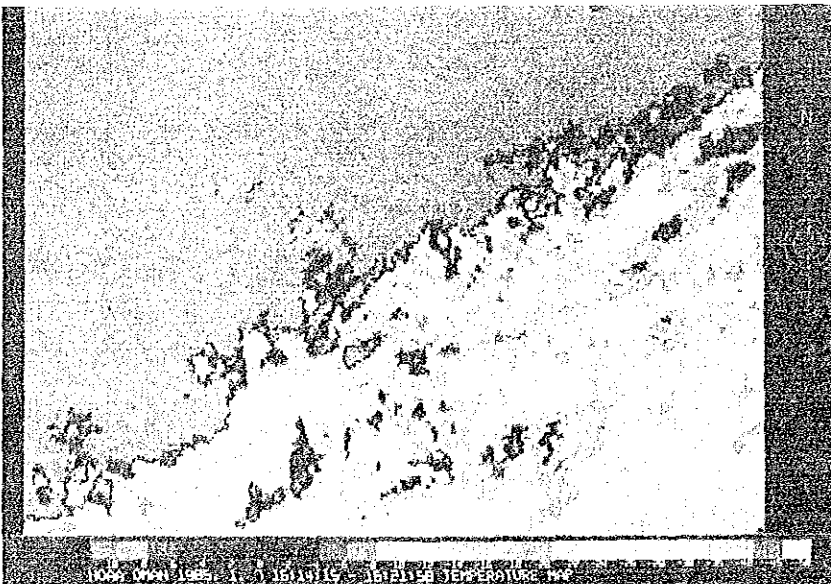
Fig. F-2-3(3) Cloud Top Temperature Distribution Image (3/3)



(a) Dec. 29, 1984



(b) Dec. 31, 1984



(c) Jan. 7, 1985

## 2.3 Features of Each Rainfall

### (1) Rainfall on August 10, 1983

- NOAA : Time when the data was collected: 03:30  
Lowest temperature at the cloud peak:  $-40^{\circ}\text{C}$
- Aerological : General wind at high altitude: ESE
- Weather : Maximum wind at altitude of 7,500 m  
(The peak of cloud at about 10,000 m according to NOAA data)

- Observation on the ground:

Four Wadi There was rainfall in the mountain from early in the morning which continued intermittently until midnight. At the coastal area, the rainfall began first in the east and moved to the west. The movement of rainfall region was about 10 km/h from east to west. The rainfall on the coastal area and the gravel field was 10 mm or less, while 88.5 mm at maximum was recorded in the mountain.

Wadi Ahin There was rainfall in the mountain from early in the morning to the next morning. On the gravel field, it began from the evening.

Because the general wind was ESE, much rainfall was observed in higher altitudes. The weather situation at that moment was strongly affected by a tropical depression on the Arabian Sea.

### (2) Rainfall on December 29, 1984

- NOAA : Time when the data was collected: 16:20  
Lowest temperature at the cloud peak:  $-40^{\circ}\text{C}$
- Aerological weather : General wind at high altitude: W  
Maximum wind at altitude of 9,400 m  
(The peak of cloud at about 10,000 m according to NOAA data)

• Observation  
on the ground:

Four Wadi      Rainfall in the mountain from afternoon continued until midnight. Maximum of 38.5 mm was recorded on the coastal area. It started late on the front mountain and the mountain with rainfall of 10 mm or less. No rainfall was recorded at six sites near the divide.

Wadi Ahin      There was rainfall on the coastal area from the afternoon to the evening. Maximum of 26.0 mm was recorded. The time rainfall began was later determined to be close to the mountain with 10 mm or less. One site recorded no rainfall.

A depression moved over Iran to the east. A cold front extending from it caused the rainfall, so that it was less in the mountain remote from the depression. When the rainfall amount and altitude of the observation sites were reviewed, it was revealed that the amount of rainfall was less as the altitude became higher, and was zero at 300 - 400 m. There was rainfall at altitudes higher than that, but it was 10 mm or less and not significant.



## 2.4 Rainfall Distribution Analysis

The appearance of rainfall itself is rare in a dry zone such as the study area, and even if when occurs, it is usually localized and short in duration.

Therefore, data was acquired after rainfall was first determined from the data of the rainfall observation sites. Thereafter one images on the day before the rainfall and two images on the day of rainfall were planned to be acquired. However, because there was problems of hardware at the NOAA Data Center, only one image on the day of the rainfall could be obtained.

Because the rainfall continues for a very short time even on a day of rainfall, the time of rainfall rarely corresponds hardly with the time when NOAA collected the data. Therefore, the plan to complement data by utilizing the NOAA data twice a day was abandoned. In the present rainfall distribution analysis, the rainfall over the entire project area was estimated by establishing the cloud brightness distribution representing the rainfall after taking into consideration conditions of rainfall at each observation site on the day of rainfall and the aerological weather situation at that moment.

Fig. F-2-3 shows the flow for the rainfall distribution analysis.

Fig. F-2-3 Flow Chart of Precipitation Distribution Analysis

